2013 Special Issue

Adaptive coupling of inferior olive neurons in cerebellar learning

Isao T. Tokuda [a,*], Huu Hoang [a], Nicolas Schweighofer [b], Mitsuo Kawato [c]

[a] Department of Mechanical Engineering, Ritsumeikan University, Shiga, Japan
[b] Biokinesiology and Physical Therapy, University of Southern California, Los Angeles, USA
[c] ATR Computational Neuroscience Laboratories, Kyoto, Japan

ARTICLE INFO

ABSTRACT

In the cerebellar learning hypothesis, inferior olive neurons are presumed to transmit high fidelity error signals, despite their low firing rates. The idea of chaotic resonance has been proposed to realize efficient error transmission by desynchronized spiking activities induced by moderate electrical coupling between inferior olive neurons. A recent study suggests that the coupling strength between inferior olive neurons can be adaptive and may decrease during the learning process. We show that such a decrease in coupling strength can be beneficial for motor learning, since efficient coupling strength depends upon the magnitude of the error signals. We introduce a scheme of adaptive coupling that enhances the learning of a neural controller for fast arm movements. Our numerical study supports the view that the controlling strategy of the coupling strength provides an additional degree of freedom to optimize the actual learning in the cerebellum.

© 2012 Elsevier Ltd. All rights reserved.

1. Introduction

1.1. Background

Intensive research on neurophysiology and theoretical modeling of the cerebellum paved the way for the establishment of the basics of the cerebellar learning (Albus, 1971; Ito, 1970; Ito, Sakurai, & Tongroach, 1982; Kawato, Furukawa, & Suzuki, 1987; Kawato & Gomi, 1992; Marr, 1969; Miall, Christensen, Cain, & Stanley, 2007; Miall, Weir, Wolpert, & Stein, 1993; Schweighofer, Spoelstra, Arbib, & Kawato, 1998; Shidara, Kawano, Gomi, & Kawato, 1993; Tseng, Diedrichsen, Krakauer, Shadmehr, & Bastian, 2007). Synaptic plasticity in parallel fiber–Purkinje cell (PC) synapses has been predicted by the learning theory of Albus (1971), Marr (1969) and Ito (1970) and was experimentally demonstrated by Ito et al. (1982). Synaptic plasticity in vestibular input synapses to central vestibular nuclei neurons has been postulated in theoretical studies (Lisberger, 1988; Raymond, Lisberger, & Mauk, 1996) and then experimentally examined in motor learning of vestibulo-ocular reflex (Highstein, Partsalis, & Arikan, 1997; Khater, Quinn, Pena, Baker, & Peterson, 1993; Pastor, De la Cruz, & Baker, 1997). Moreover, synaptic plasticity at mossy fiber–granule cell relay has been observed in experiment (D'Angelo, Rossi, Armano, & Taglietti, 1999) and implemented in a computational model (Schweighofer, Doya, & Lay, 2001). Among these studies, the most famous form of the cerebellar learning is based upon long-term synaptic changes induced at the PCs, which output motor commands to the cerebellar nuclei (CN) while receiving two types of major excitatory inputs: >100,000 parallel fibers from granule cells and a sole but powerful climbing fiber input from inferior olive (IO). Whereas the granule cells transmit signals from the sensory system and the cerebral cortex, the IO neurons were found to send error signals (Gilbert & Thach, 1977; Kitazawa, Kimura, & Yin, 1998). When conjointly activated at the PCs, these two inputs cause a long-term depression (LTD), reducing the efficacy of the synaptic transmission in the parallel fiber (Ito et al., 1982).

1.2. Chaotic resonance

Structures and functions of the cerebellum have been modeled in a variety of artificial learning machines such as a cerebellar model for articulation controller (Albus, 1975), which learns inverse or forward models from errors. In the supervised learning of the artificial machine, synaptic connections from the granule cells to the PCs are modified by minimizing the errors carried through the climbing fibers. The main difference between the learning machine and the biological system is that, in the real cerebellum, the error signals are carried by the IO neurons, whose firing rate is very low, with typically a single or two spikes per movement. This provides a severe limit of precisely transmitting the error signals with high temporal resolution in contrast to the artificial machine, which is capable of transmitting any high frequency component of the error signals.

* Corresponding author. Tel.: +81 77 561 2832; fax: +81 77 561 2665.
E-mail address: isao@fc.ritsumei.ac.jp (I.T. Tokuda).

Concerning this problem, a network of IO neurons may play a key role. As far as the IO neurons are activated in a synchronous manner, an ensemble of IO neurons behaves as a single neuron, which does not help overcome the limited capability of the error transmission. However, if the IO neurons operate asynchronously, the spike timings of each neuron are scattered to increase the time resolution of the population coding of the error signal. Here, it is natural to consider that the level of synchrony between the IO neurons is regulated by the electrical coupling by gap junctions (De Zeeuw et al., 1998; Llinás, Baker, & Sotelo, 1974). If the coupling strength is too strong, it induces coherent IO activities. If the coupling is too weak, on the other hand, common input stimuli entrain the IO neurons, resulting again in their coherent activities. In contrast, intermediate strength of the electrical coupling was found to induce irregular or even chaotic spikes, which effectively desynchronize the IO activities and thus optimize the population coding (Schweighofer et al., 2004). The advantages of desynchronized firing activities were discussed in an abstract and a general framework (Masuda & Aihara, 2002, 2003). By distributing the frequency components of the error signal over sporadic, irregular, and non-phase-locked spikes, the temporal resolution of the error transmission is significantly improved. The Purkinje cells can then reconstruct the complete error signal via spatio-temporal integration of the IO cell activities. Since optimal learning is realized with an intermediate coupling strength that maximizes the level of the chaotic activity, this hypothesis has been termed as *chaotic resonance*. The idea of chaotic resonance has been examined so far for IO networks for information transmission (Schweighofer et al., 2004) as well as for a feedback-error learning of multi-joint arm control (Tokuda, Han, Aihara, Kawato, & Schweighofer, 2010).

1.3. Learning in early and late stages

Despite such intensive studies, important open questions remain on the chaotic resonance. For instance, it is still unclear how to tune the coupling strength of the IO neurons into a certain range so that an efficient learning takes place. Although the coupling strength has been assumed to be fixed to a constant level, there have been several physiological studies suggesting that the formation of synchronously firing IO neurons is a dynamic process and that the coupling can be modulated by inhibitory inputs from the cerebellar nucleus (Best & Regehr, 2009; Lang, Sugihara, & Llinás, 1996; Llinás et al., 1974; Uusisaari & De Schutter, 2011). Moreover, a recent study (Kawato, Kuroda, & Schweighofer, 2011) proposed a functional role of a triangle circuit of IOs, PCs, and CN, which may change the effective strength of the IO coupling during the motor learning (Fig. 1). In this circuit, PCs inhibit the activity of the CN cells, which provide inhibitory synapses on the dendritic spines that form electrical connections between neighboring IO neurons (Oniuzka et al., 2013; Onizuka et al., 2010). In the early stage of learning, since the executed behaviors deviate from the desired ones, plans and motor commands are strongly modulated and the error signals should be large. This activates the PC cells, which then strongly suppress the CN cells. The suppressed CN cells deactivate their inhibitory shunting effects on the IO coupling, and therefore the IO neurons are strongly electrically coupled. In contrast, in the late stage of learning, the executed movements become smooth and get close to the desired ones. Then the input signals to the PCs and the error signals are weakened. Since the PCs are weakly activated, the CN cells are only weakly suppressed. Because of the strong inhibitory effects from the active CN cells, the electrical coupling between the IO neurons is weakened. In this way, the coupling strength between the IO neurons can be modulated during the learning process.

1.4. Adaptive coupling to control inferior olive activities

The aim of the present paper is to examines the idea of adaptive coupling in cerebellar learning. In accordance with the hypothesis of Kawato et al. (2011), the coupling strength between IO neurons is slowly decreased as the learning proceeds. We examine the advantage of the adaptive coupling over conventional situations, in which the coupling strength is fixed to a constant level during the entire learning. We focus on the basic property of chaotic resonance, which is in principle an interplay between synchronization of the IO neurons induced by error signals and destruction of the synchronized IO activities by chaos. In motor learning, a group of IO neurons receives an error signal as a common external forcing. In the study of coupled oscillators, it is well known that such a common force entrains the activities of the IO neurons, and as a result of the entrainment, the neurons are synchronized (Goldobin, Teramae, Nakao, & Ermentrout, 2010; Pikovsky, Rosenblum, & Kurths, 2001; Teramae & Tanaka, 2004). On the other hand, an intermediate coupling between the IO neurons can induce chaotic dynamics that destroys the synchronized neural activities (Fujii & Tsuda, 2004; Tsuda, Fujii, Tadokoro, Yasuoka, & Yamaguchi, 2004). The balance between the neuronal synchrony and its destruction is the key factor of the chaotic resonance. This feature can be combined with the idea of adaptive coupling. Namely, in the beginning of the learning, the error signals are so large that they strongly entrain the IO neurons. To destroy such a strong synchrony, an intermediate coupling strength is required to effectively produce chaotic dynamics. On the other hand, in the late stage of learning, the error signals become weak and do not strongly influence the IO neurons. Without much entrainment to the error signal, no strong coupling is required to destroy the synchronized activities of the IO neurons. This represents a design principle for the optimal control of the coupling in cerebellar learning.

The present paper is organized as follows. First, to study the basic properties of the network of IO neurons, we analyze its capability of information transmission using an artificial signal as an input to an IO network. The optimal coupling strength is shown to depend upon the strength of the input signal; strong input requires intermediate coupling, whereas weak input requires only weak coupling. Then this idea is applied to the control problem of a multi-joint arm, where a model of the IO neurons is implemented to transmit the error signals in feedback-error learning. In accordance with the basic property of efficient information transmission, the optimal coupling strength depends again upon the strength of the error signal. As a final study, we designed a control scheme for the adaptive coupling to slowly decrease its strength as the learning proceeds. Such adaptive coupling is shown to be more efficient than the situation in which the coupling strength is fixed during the entire learning.

2. Methods

2.1. Inferior olive model

Following our previous study (Tokuda et al., 2010), the dynamics of IO neurons are described by the μ-model (Fujii & Tsuda, 2004; Tsuda et al., 2004), which generates a limit cycle oscillation under an isolated condition, whereas it gives rise to complex chaotic activity through gap-junction connections with other neurons. These properties reproduce the basic activity of IO neurons known from physiological and modeling studies (Katori, Lang, Onizuka, Kawato, & Aihara, 2010; Lang et al., 1996; Llinás & Yarom, 1981a, 1981b, 1986; Makarenko & Llinás, 1998; Manor, Rinzel, Segev, & Yarom, 1997; Schweighofer et al.,
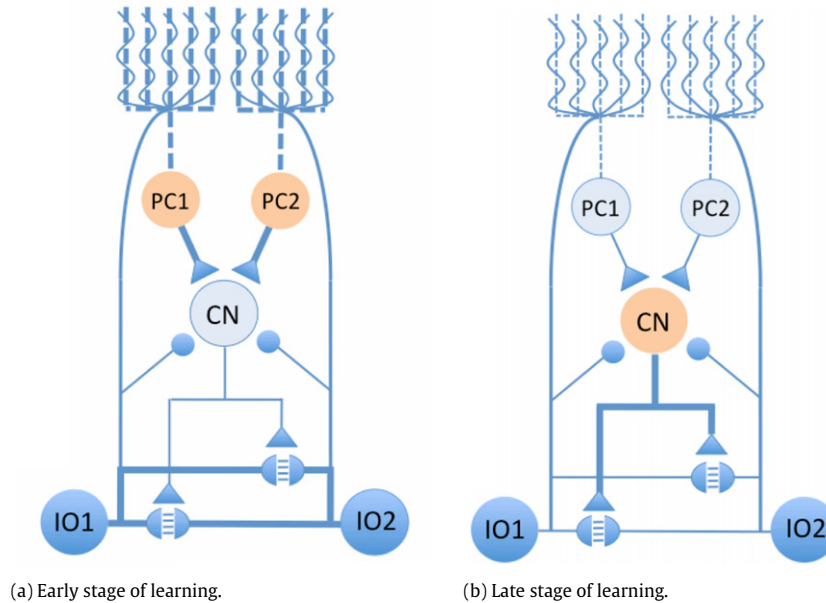
Fig. 1. Schematic illustration for possible functions of a triangle circuit consisting of inferior olive (IO), Purkinje cell (PC), and cerebellar nucleus (CN). PCs inhibit CN cell activity, whereas CN cells provide an inhibitory effect on synaptic connections of IO neurons. (a) In the early stage of learning, since the executed trajectories are far from the desired ones, plans and motor commands highly modulate PCs, and thus the excited PCs suppress CN cells. Since an inhibitory synaptic effect from the CN cells is not activated, IO neurons are strongly coupled. (b) In the late stage of learning, since the movements become smooth and close to the desired ones, inputs to PCs become weak. Since weakly modulated PCs do not strongly suppress CN cells, inhibitory synaptic effect from the CN cells is activated and, coupling of IO neurons is weakened.

2004; Schweighofer, Doya, & Kawato, 1999). A network of locally connected μ-neurons is given by:

$$\eta_i \frac{dx_i}{dt} = -y_i - \mu x_i^2 \left(x_i - \frac{3}{2} \right) + I + J_i,$$
$$\eta_i \frac{dy_i}{dt} = -y_i + \mu x_i^2,$$

(1)

where

$$J_i = \begin{cases} g(x_2 + x_N - 2x_1) & (i = 1) \\ g(x_{i+1} + x_{i-1} - 2x_i) & (i = 2, \dots, N-1) \\ g(x_1 + x_{N-1} - 2x_N) & (i = N). \end{cases}$$

(2)

Here x_i and y_i represent the membrane potential and the ion channel activity of the ith neuron ($i = 1, 2, \dots, N$), N is the total number of neurons, η_i is a time constant of the ith neuron, μ is a system parameter, g is the strength of the electrical coupling, and I is an external input. Compared to our previous study (Tokuda et al., 2010), the μ parameter was set to be the same for all the neurons. Instead, time constant η_i was set differently to each neuron to describe the heterogeneity of the IO neurons. Since the time constant determines the oscillation frequency of each neuron, this heterogeneity gives rise to asynchronous firing of the neurons when they are weakly coupled.

The spiking activity of the kth IO neuron is defined as a membrane potential that exceeds a threshold value of x_{th}. In the following simulations, Eqs. (1) and (2) were integrated by the 4th order Runge–Kutta algorithm from a random initial condition, where 20 simulations were run to compute the average quantities to determine the dependence of the neural dynamics on the random initial conditions.

2.2. Capability of information transmission

To examine the basic property of the network of IO neurons, we evaluated its capability of information transmission by computing the mutual information, which is a quantity to measure mutual dependence of two random variables (Rényi, 1970). If the two random variables are independent, the mutual information becomes zero. If the two random variables are identical, on the other hand, the mutual information is equal to the entropy of the random variable. Larger mutual information means that the two variables are more strongly dependent upon each other.

Here, each neuron receives a common input signal, whereas their spiking activities are temporally and spatially integrated as the output response. The mutual information between the input signal and the output response is measured. As an input signal, a chaotic signal is generated from the Rössler equations ($\tau \dot{x} = -y - z$, $\tau \dot{y} = x + 0.36y$, $\tau \dot{z} = 0.4x - (4.5 - x)z$, $\tau = 1/0.22$) (Rössler, 1979), where the y-variable is injected to all the neurons as $I = I_0 + \beta y$. I_0 and β stand for the minimal input and the input gain, where the minimal input is set as $I_0 = 0.01$. Output $S(t)$ represents the number of spikes generated from the network of neurons within a time interval of 0.02 at time t. To compute the mutual information between input $I(t)$ and output $S(t)$, the signals are discretized into 25 bins for calculating the probability distributions. Note that one of the key parameters is given by input gain β, which determines the strength of the input signal. Our interest is to compare the neural responses for a strong input ($\beta = 0.002$) and a weak input ($\beta = 0.0004$).

2.3. Quantification of synchrony

The capability of information transmission is dependent upon the degree of the synchronized activities of the IO neurons (Masuda & Aihara, 2002, 2003; Schweighofer et al., 2004). If the network of neurons is strongly synchronized, their activity is essentially the same as that of a single neuron, which severely limits the signal transmission because of the low firing frequency of the IO neuron. As an index to measure the synchronized neural activity, we computed order parameter R (Kuramoto, 1984). The order parameter, which is defined as $R \exp(i\Phi) = (1/N) \Sigma_{j=1}^{N} \exp(i\phi_j)$ using the phase of the jth neuron given by angle $\phi_j = \arctan(\frac{y_j - 0.10}{x_j - 0.05})$, takes a real value between 0 and 1, where a large value close to $R = 1$ implies strong mutual synchronization and a small value close to $R = 0$ implies desynchronization.

2.4. Quantification of chaotic activity

In the chaotic resonance hypothesis, chaotic dynamics plays an important role in destroying the synchronized activity of IO neurons. To quantify the strength of the chaotic activity, we calculated the Lyapunov dimension. The Kaplan–Yorke formula (Kaplan & Yorke, 1970) defines the Lyapunov dimension as $D_L = k + \sum_{i=1}^{k} \lambda_i / |\lambda_{k+1}|$, where $\lambda_1 \geq \lambda_2 \geq \cdots \geq \lambda_{2N}$ stand for the Lyapunov exponents, which are computed by the Shimada–Nagashima algorithm (Shimada & Nagashima, 1979), and k is the maximal value of j such that $\sum_{i=1}^{j} \lambda_i \geq 0$. The Lyapunov exponent measures the separation speed of the nearby orbits in a state space. A positive Lyapunov exponent implies chaos, which exponentially expands the distance of the nearby orbits. The Lyapunov dimension roughly measures the effective number of positive Lyapunov exponents.

2.5. Feedback-error learning of multi-joint arm

We examined the function of IO neurons as a transmitter of error signals in an idealized model of the cerebellum that learns an inverse model of an arm movement by feedback-error learning (Kawato et al., 1987; Kawato & Gomi, 1992; Schweighofer et al., 1998; Shidara et al., 1993). In feedback-error learning, the supervised learning of a feedforward controller occurs using a feedback control signal as the error signal. Since we focus mainly on the function of IO neurons, we only modeled the minimal entities of the cerebellum and considered the functions of PCs, granule cells, and IO neurons as in previous works (Schweighofer et al., 2001; Tokuda et al., 2010).

It has been suggested that functionally related PCs, CN cells, and IO neurons are grouped into *micro-complexes* or modules (Apps & Hawkes, 2009; Ito, 1984, 1990; Marshall & Lang, 2009; Schweighofer, 1998). Within each micro-complex, population of IO neurons is coupled by gap junctions to form a closed network. For simplicity, the network of IO neurons is considered to be independent from networks of other micro-complexes. In each micro-complex, a group of PCs projects to synergetic muscles of a joint in the arm. Since we modeled a two-joint arm consisting of elbow and shoulder, we constructed two micro-complexes, each of which controls elbow or shoulder joint.

In our simulation, the granule cells receive a desired state in joint space instead of sensory input from the mossy fibers because of the following reason (Schweighofer et al., 2001). It has been known that the mossy fibers have two origins: a cell originating from the cerebral cortex and a sensory cell (Van Kan, Gibson, & Houk, 1993). The mossy fibers of the central origin are considered to carry information about the desired trajectory. Because there are no delays and no noise in the model, the desired and sensed trajectories become quite similar after the learning. Moreover, because of the function of the cerebral feedback controller, they are not so different even during the learning. Thus, for simplicity, we assumed in the present model that all inputs to the mossy fibers are of central origin.

The granule cells receive the mossy fiber inputs with fixed random weights and are projected to PCs through parallel fibers. The IO neurons transmit the feedback error signals to the PCs, where the learning takes place to modify the efficacy of the synaptic transmission in the parallel fiber. In the Appendix, the details of the feedback-error learning and the simulation conditions are described.

As a brief description of the IO model, feedback commands u_{fb}, which represent the error signals in the feedback-error learning (Eq. (A.3) in the Appendix), are injected to the IO neurons as $I = I_0 + \beta \cdot u_{fb}$. The spiking activities of the IO neurons are then used as error signals to modify the synaptic plasticity between the granule
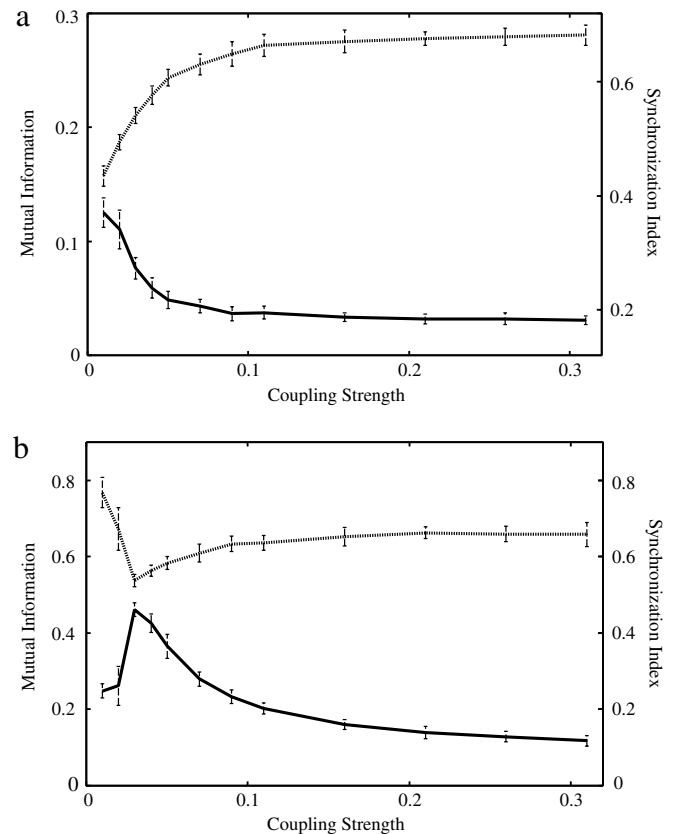
Fig. 2. Mutual information (solid line) and synchronization index (dotted line) of a network of IO neurons receiving a chaotic signal. Coupling strength is varied in range of $g \in [0, 0.3]$. Error bars stand for a standard deviation over twenty simulations starting from random initial conditions. (a) Input signal is weak ($\beta = 0.0004$). (b) Input signal is strong ($\beta = 0.002$).

cells and the PCs. Since the input gain β determines the forcing strength of the IO neurons, it provides an important parameter to control the synchronized IO activity.

3. Results

3.1. Information transmission

The mutual information and the synchronization index were calculated for a network of IO neurons. The coupling strength was varied in the range of $g \in [0, 0.3]$. Fig. 2(a) shows the case of a weak input ($\beta = 0.0004$), while Fig. 2(b) shows the case of a strong input ($\beta = 0.002$). In the case of the strong input, the synchronization index was relatively high in the weak coupling regime. As the coupling strength increased, the synchronization index decreased and took a minimal value at around $g = 0.04$. Further increase in the coupling strength monotonically increased the synchronization index. The mutual information is inversely proportional to the synchronization index. The mutual information peaked around $g = 0.04$ and decreased as the coupling increased or decreased from the peak. This relationship is reasonable, because the desynchronized activity of the IO neurons enhances the capability of information transmission. The synchronized activity was high for both weak and strong coupling because of the entrainment effect induced by the input signal and the coupling effect between the IO neurons, respectively. The Lyapunov dimension, on the other hand, peaked around $g = 0.045$ (Fig. 3), which is near the minimum point of the synchronization index. This implies that chaotic dynamics most efficiently destroyed the synchronized activity of the IO neurons
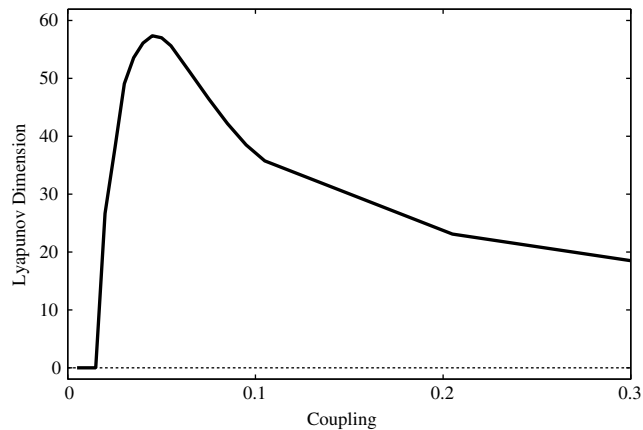
Fig. 3. Lyapunov dimension D_L computed from a network of IO neurons. Coupling strength is varied in range of $g \in [0, 0.3]$.

when the Lyapunov dimension was maximized. This is in good agreement with the chaotic resonance hypothesis.

The situation is different for the weak input (Fig. 2(a)). The synchronization index increased monotonically as the coupling increased; no peak was discernible. This is because the input signal was not strong enough to entrain the IO neurons to achieve synchrony and chaos played no role to destroy the synchronous neural firings. For this reason, the peak in the Lyapunov dimension did not produce any peak in the mutual information.

To clarify the relationship between the mutual information, the synchronization index, and the Lyapunov dimension, we computed the correlation coefficients. For strong input, the correlation coefficient between the mutual information and the synchronization index was -0.67 ($p = 0.007$), whereas between the mutual information and the Lyapunov dimension it was 0.74 ($p < 0.001$). For weak input, the correlation coefficient between the mutual information and the synchronization index was -0.98 ($p < 0.001$), but between the mutual information and the Lyapunov dimension it was -0.31 ($p > 0.1$). This indicates that synchrony is always correlated with mutual information, whereas chaos is correlated with mutual information only when the input signal is strong.

3.2. Feedback-error learning

When the input error signals to the IO neurons are weak ($\beta = 0.001$), we examined the efficiency of the feedback-error learning. Fig. 4(a) compares two learning curves corresponding to weak coupling ($g = 0.001$) and intermediate coupling ($g = 0.05$). The error bars represent standard deviations over twenty simulations starting from random initial conditions. The weak coupling produced an averaged error curve lower than that of the intermediate coupling. The dependence of the learning error at 10th step on the coupling strength is further displayed in the range of $g \in [0, 0.15]$ in Fig. 5(a). The error, which was relatively small for weak coupling, monotonically increased as the coupling strength increased. The synchronization index also increased monotonically as the coupling strength increased. This implies that increased coupling strengthened the synchronization of the IO activities, which lowered the efficiency of the error transmission and thus slowed down the learning.

Next, we focus on the case where the input signals to the IO neurons are relatively strong ($\beta = 0.05$). As shown in Fig. 4(b), the learning curve of the intermediate coupling ($g = 0.05$) took smaller errors than the weak coupling ($g = 0.001$). Compared to Fig. 4(a), the situation is reversed. The dependence of the learning error at 10th step on the coupling strength indicates that the error
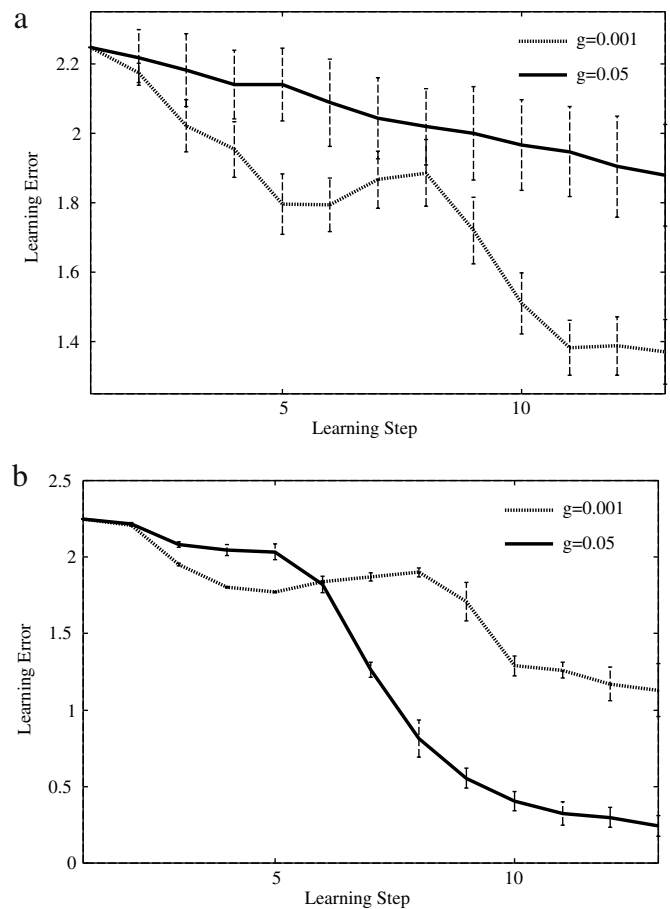
Fig. 4. Learning error curves obtained from network of IO neurons with $g = 0.001$ (dotted line) and $g = 0.05$ (solid line). (a) Input signal is weak ($\beta = 0.001$). (b) Input signal is strong ($\beta = 0.05$).

took a small value in the range of $g \in [0.05, 0.1]$ (Fig. 5(b)). The synchronization index showed a similar tendency and took a small value around $g = 0.05$. This minimum is located close to where the Lyapunov dimension is maximized, implying that chaotic dynamics destroyed the synchronous IO activity, improved the transmission of the error signal, and enhanced the learning.

Case studies of both strong and weak input signals indicated that the optimal coupling strength to realize efficient learning depends upon the strength of the input error signals. As shown in Fig. 6, coupling strength that gives rise to minimum error was shifted from a small value to a large one as the input gain increased.

As a final simulation, Fig. 7(b) shows the learning curve of the adaptive coupling. The input gain was set as $\beta = 0.013$. At the beginning of the learning, the coupling strength was set to be $g = 0.05$, and it was reduced to $g = 0.01$ as the learning proceeded (solid line of Fig. 7(a)). Compared with the cases where the coupling strength was fixed to a constant value of $g = 0.01$ or $g = 0.05$, the adaptive coupling showed an error curve smaller than those of the fixed couplings.

4. Conclusions and discussions

To summarize, we used a simple model to study the function of IO neurons in cerebellar learning to determine how coupling strength, which gives rise to efficient learning, depends upon the strength of the error signals. First, to examine the capability of the information transmission, an artificial signal was injected into a network of IO neurons. By varying the coupling strength, mutual information between the input signal and the output responses of

a

b
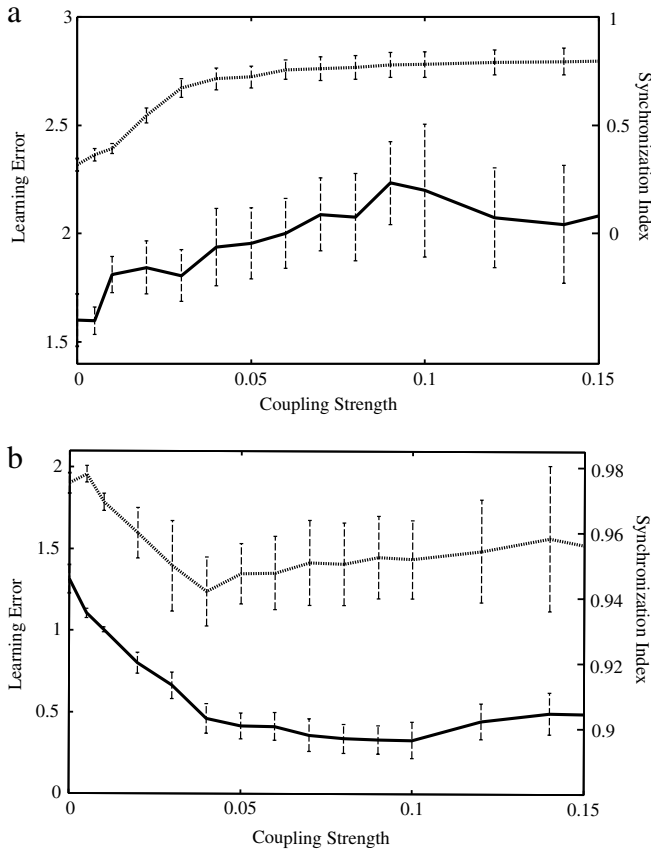
Fig. 5. Dependence of learning error (solid line) recorded at 10th step on coupling strength ($g \in [0, 0.15]$). Corresponding synchronization index (dotted line) is simultaneously drawn. (a) Input signal is weak ($\beta = 0.001$). (b) Input signal is strong ($\beta = 0.05$).
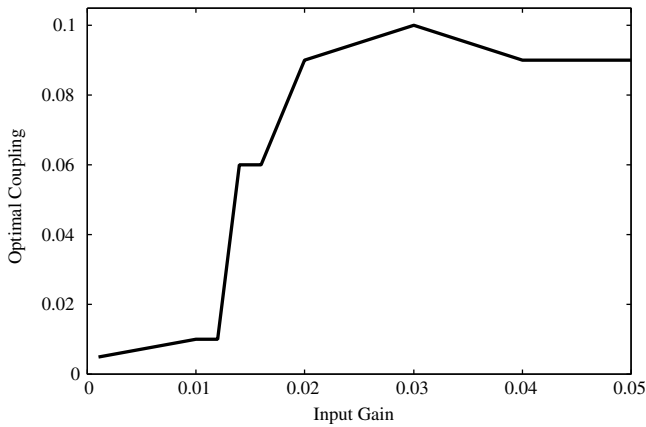
Fig. 6. Dependence of coupling strength that minimizes learning error on input gain $\beta \in [0, 0.05]$.

the IO network was computed. The synchronization index highly correlated with the mutual information (Fig. 2(a) and (b)), because desynchronized activities of IO neurons are essential for efficient information transmission (Schweighofer et al., 2004). When the input signal is strong, the synchronized activity of the IO neurons was enhanced due to their entrainment to the strong input signal. This produces a large synchronization index in the weak coupling regime (Fig. 2(b)). The synchronized IO activities were destroyed with an intermediate coupling that produces a strong chaotic activity. Since chaos is important to destroy synchrony to enhance the information transmission, the Lyapunov dimension highly correlated with the mutual information.

a

b
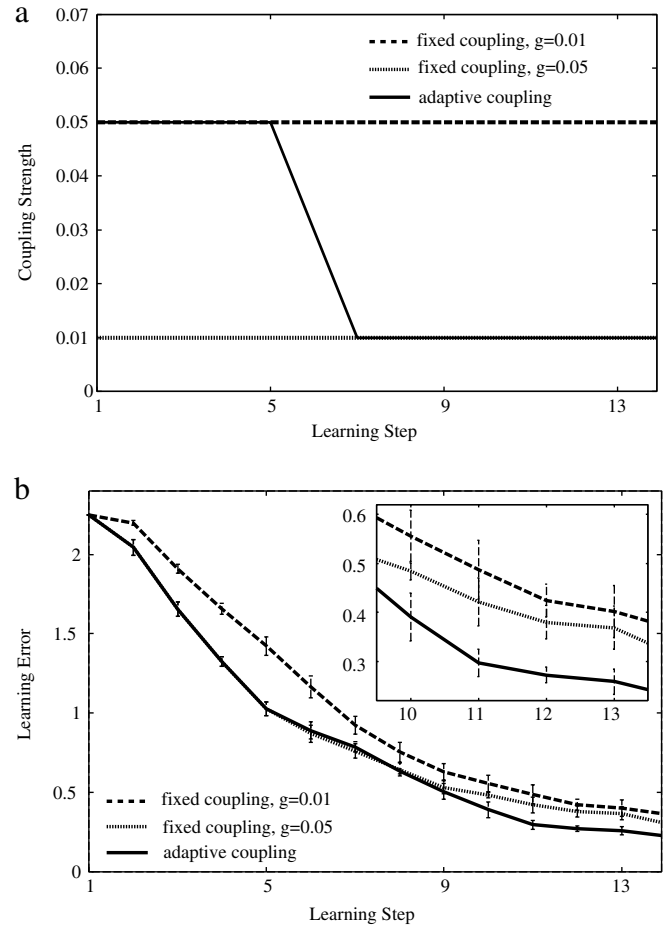
Fig. 7. (a) In adaptive coupling, coupling strength is initially set to $g = 0.05$ and decreased to $g = 0.01$ as learning proceeds. (b) Learning error curves obtained from network of IO neurons with adaptive coupling (solid line), fixed coupling of $g = 0.01$ (dashed line), and fixed coupling of $g = 0.05$ (dotted line). In a small box, error curves are enlarged in range of learning steps from 10 to 13.

When the input signal is weak, highly synchronized activity of the IO neurons was not observed in the weak coupling regime (Fig. 2(a)) because the input signal was not strong enough to entrain the IO neurons. Here, since chaos played no role in destroying the synchronous neural firings, the Lyapunov dimension was not correlated with the mutual information.

These observations lead to the first part of our conclusion that the balance between neuronal synchrony and its destruction is the key factor to determine the optimal coupling strength. A strong input signal that enhances neural synchrony requires an intermediate coupling to destroy the synchrony, whereas a weak input signal that does not enhance the neuronal synchrony requires only weak coupling, which suffices to support desynchronized IO activities.

In the second part of our study, we applied adaptive coupling to the control problem of a multi-joint arm, where a model of the IO neurons was implemented to transmit the error signals in the feedback-error learning. In accordance with the basic property of information transmission, the optimal coupling strength depended again upon the strength of the error signal. For a strong error signal, intermediate coupling strength effectively lowered the synchronous IO activity that accurately transmitted the error signal and enhanced motor learning (Fig. 5(b)). On the other hand, for a weak error signal, weak coupling was enough to realize desynchronized IO activities that enhanced motor learning (Fig. 5(a)).

In the final simulation, we designed an adaptive control to slowly decrease the coupling strength as the learning proceeded (Fig. 7(a)) based on the following expectation. In the beginning of the learning, the error signals are large, because an untrained system produces undesired movements. Strong coupling is required to destroy the neuronal synchrony induced by such large error signals. As the learning proceeds, the system movement becomes close to the desired one and the error signals become smaller. Since the small error signals only weakly influence the IO neurons, weak coupling is sufficient to maintain the desynchronized neural activities. This scenario was confirmed and the adaptive coupling was shown to be more efficient than the situation in which the coupling strength was fixed during the entire learning (Fig. 7(b)). Note that, in the adaptive control, the coupling strength was changed rather abruptly from a large value to a small one (Fig. 7(a)). This is due to the property of the learning system, whose optimal coupling location quickly switches from a large value to a small one around the region of $\beta \in [0.01, 0.02]$ (Fig. 6). Such a rapid switch implies that the coupling should also be decreased quickly as soon as the error signals are weakened in the learning process. The controlling scheme of the coupling should be designed in such a way to adapt to the inherent property of the learning system in the cerebellum.

The present adaptive coupling scheme is supported by the recent hypothesis of Kawato et al. (2011) who focused on the physiological functions of the closed triangle circuit of IO–PC–CN, which may control the coupling strength of the IO neurons (Fig. 1). In the early stage of learning, the PCs are strongly modulated by motor commands. The modulated PCs inactivate the inhibitory effect of the CN cells on the IO coupling. Thus the IO neurons are initially strongly coupled. In contrast, in the late stage of learning, the PCs are only weakly modulated and hardly inactivate the inhibitory effect of the CN cells. This weakens the coupling strength of the IO neurons. The hypothesis therefore implies that, in the actual cerebellar learning, the coupling strength is adaptive and should be weakened as the learning proceeds. The present study demonstrated that such an adaptive control of the coupling is quite beneficial in the motor learning.

The role of electrical coupling in cerebellar learning has been confirmed by recent experiments on mice mutants lacking electrical coupling between the IO neurons. Although these mice show no general motor deficits, they exhibit deficits in learning-dependent motor tasks such as locomotor or eye-blink conditioning (Van Der Giessen et al., 2008). The authors suggested that the electrical coupling among the IO neurons by gap junctions is essential for proper timing of their action potentials and for learning-dependent timing in cerebellar motor control. Similarly, humans with reduced or no IO coupling exhibit no general motor deficits but show motor learning impairments (Van Essen et al., 2010). Our hypothesis of the adaptive coupling may provide additional explanation on these learning deficits.

Our idea is distinguished from the related function of the IO circuitry. It has been known that a CN–IO pathway can function as a negative feedback loop, in which the CN inhibits the IO firing through GABA (Andersson, Garwicz, & Hesslow, 1988; De Zeeuw et al., 1996; Hesslow, 1986; Nelson & Mugnaini, 1989). The cerebellar learning can be regulated by this negative feedback (Bengtsson & Hesslow, 2006; Best & Regehr, 2009; De Zeeuw et al., 1998; Lang et al., 1996; Marshall & Lang, 2009). For instance, through interactions between excitatory and inhibitory inputs, the negative feedback system may selectively transmit error signals when they are needed and inhibit them when the signals should be blocked (Andersson & Armstrong, 1987; Apps, Atkins, & Garwicz, 1997; Gellman, Gibson, & Houk, 1985; Hesslow & Ivarsson, 1996; Kim, Krupa, & Thompson, 1998; Lidierth & Apps, 1990). The blocking of the teaching pathway is also considered to play an important role in the reinforcement learning for

classical conditioning of discrete responses such as associative eyeblink conditioning (Hesslow & Ivarsson, 1996; Kim et al., 1998; Thompson, Thompson, Kim, Krupa, & Shinkman, 1998). In contrast to such a strong blocking function, our scheme does not directly inhibit the input signals, but it tunes the coupling strength to control the capability of information transmission of the IO neurons. In this sense, our focus is more on a delicate level of regulating the error signals.

Finally, we note that the original scenario of Kawato et al. (2011) further discussed the possibility of degrees-of-freedom control. Here, strong initial coupling may induce highly synchronized activities of IO neurons and PCs, reducing the number of independently firing PCs. They have conjectured that such low degrees-of-freedom can be advantageous for avoiding local minima and increasing learning speed. As learning proceeds, weakened coupling may reduce the synchronized activities of the IO neurons and the PCs and they may exhibit complex dynamics with full degrees-of-freedom. Such high degrees-of-freedom can be useful for slow but sophisticated learning in the late stage. The present study did not consider such an initially strong coupling that may control the degrees-of-freedom of the IO–PC–CN circuit. We only focused on coupling strength ranging from small to intermediate levels. Future work takes into account the degrees-of-freedom control in the cerebellar motor learning.

Acknowledgments

Appendix

This Appendix provides a basic framework of the feedback-error learning of a multi-joint arm and details of the simulation conditions. As a model for a multi-joint arm, we utilized a two-link human arm on a horizontal plane and adapted parameters from Katayama and Kawato (1993). The equation of motion for the arm movement is given by

$$\mathbf{M}(\theta)\ddot{\theta} + \mathbf{C}(\dot{\theta}, \theta)\dot{\theta} = \tau, \tag{A.1}$$

where θ is a vector of the arm joint angles and τ is a motor command. Inertial and Coriolis matrices M and C are given by

$$M_{11} = I_1 + I_2 + 2W_2L_1\cos(\theta_e) + W_1L_1^2,$$
$$M_{12} = M_{21} = I_2 + W_2L_1\cos(\theta_e), M_{22} = I_2,$$
$$C_{11} = -2W_2L_1\sin(\theta_e)\dot{\theta}_s,$$
$$C_{12} = -W_2L_1\sin(\theta_e)\dot{\theta}_e = -C_{21}, C_{22} = 0,$$

where θ_e is an elbow joint angle, θ_s is a shoulder joint angle, L_1 and L_2 are segment lengths, I_1 and I_2 are inertia parameters, and W_1 and W_2 are two other parameters.

In feedback-error learning, the outputs of a crude feedback controller and a feedforward controller are summed to form the motor command. The controller receives a desired minimum jerk trajectory (Flash & Hogan, 1985) in the joint coordinates. The vectors of the motor commands are given by the sum of feedback ufb and feedforward motor commands uff as:

$$\tau = ufb + uff. \tag{A.2}$$

The feedback commands are given by the proportional derivative (PD) control as

$$ufb = K_P \cdot (\theta_d - \theta_{\text{sensed}}) + K_D \cdot (\dot{\theta}_d - \dot{\theta}_{\text{sensed}}), \tag{A.3}$$

where θ_d and θ_{sensed} are the vectors of the desired and actual joint position. Note that ufb represents an error signal, which is used

both for feedback control and as input to the IO. The IO trains the feedforward controller composed of a network of a "granule cell" layer, which sends its output to a "Purkinje cell" layer:

$$GC_j = \tanh\left(\sum_i v_{ji}s_i\right), \tag{A.4}$$

$$PC_k = \sum_j w_{kj}GC_j, \tag{A.5}$$

where GC_j is the jth granule cell activity, PC_k is the kth PC activity, v represents the fixed weights from the inputs to the granule cells, w represents the modifiable weights from the granule cells to the PCs, and input $s = [\theta_e, \theta_s, \dot{\theta}_e, \dot{\theta}_s, \ddot{\theta}_e, \ddot{\theta}_s]$ represents the desired state vector.

The weights from the granule cells to the Purkinje cell layer are updated based on a simplified model of synaptic plasticity between the granule cells and the PCs (Kawato & Gomi, 1992):

$$w'_{kj} = w_{kj} + \alpha \cdot (IO_k - IO_{mean}) \cdot GC_j, \tag{A.6}$$

where IO_k is the spiking activity of the kth IO neuron and α is a learning rate. Before learning, mean firing rate IO_{mean} is determined by averaging the mean firing rates over all the IO neurons with constant input $I = I_0$.

The motor task is to reach a target located at $[0.1, 0.3]$ m starting from $[-0.1, 0.3]$ m with a movement time of 0.6 s. The shoulder is located at $[0, 0]$. During each learning trial, the feedback command is integrated as learning error. 100 granule cells send their inputs to 50 PCs for each joint, where 50 IO neurons per joint are connected to the PCs in one-to-one fashion. The fixed weights from the desired state to the granule cells layer are initialized by random variables $N(0, 1)$, and the modifiable weights from the granule cell to the Purkinje cell layer are initialized to zero. In the IO models, the μ-parameter is set to $\mu = 1.65$, which has been reported as plausible for spiking neurons (Fujii & Tsuda, 2004; Tsuda et al., 2004). Time constants η_i are set randomly to each IO neuron as $\eta_i \in [0.035, 0.045]$, which realizes a low firing frequency of about 2 Hz for a constant input. Other simulation parameters are given as $x_{th} = 0.75, I_0 = 0.2, \alpha = 0.02, L_1 = 0.33$ m, $L_2 = 0.34, I_1 = 0.067$ kg m^2, $I_2 = 0.97$ kg m^2, $W_1 = 1.52$ kg, and $W_2 = 0.34$ kg m, $K_P = 100, K_D = 1$, and time step $dt = 0.003$.

References

Albus, J. S. (1971). The theory of cerebellar function. *Mathematical Biosciences*, *10*, 25–61.

Albus, J. S. (1975). A new approach to manipulator control: the cerebellar model articulation controller (CMAC). *Journal of Dynamic Systems, Measurement, and Control*, *97*, 270–277.

Andersson, G., & Armstrong, D. M. (1987). Complex spikes in Purkinje cells in the lateral vermis (b zone) of the cat cerebellum during locomotion. *Journal of Physiology*, *385*, 107–134.

Andersson, G., Garwicz, M., & Hesslow, G. (1988). Evidence for a GABA-mediated cerebellar inhibition of the inferior olive in the cat. *Experimental Brain Research*, *72*, 450–456.

Apps, R., Atkins, M. J., & Garwicz, M. (1997). Gating of cutaneous input to cerebellar climbing fibres during a reaching task in the cat. *Journal of Physiology (London)*, *502*, 203–214.

Apps, R., & Hawkes, R. (2009). Cerebellar cortical organization: a one-map hypothesis. *Nature Reviews Neuroscience*, *10*(9), 670–681.

Bengtsson, F., & Hesslow, G. (2006). Cerebellar control of the inferior olive. *Cerebellum*, *5*, 7–14.

Best, A. R., & Regehr, W. G. (2009). Inhibitory regulation of electrically coupled neurons in the inferior olive is mediated by asynchronous release of GABA. *Neuron*, *62*(4), 555–565.

D'Angelo, E., Rossi, P., Armano, S., & Taglietti, V. (1999). Evidence for NMDA and mGlu receptor-dependent long-term potentiation of mossy fiber–granule cell transmission in rat cerebellum. *Journal of Neurophysiology*, *81*, 277–287.

De Zeeuw, C. I., Lang, E. J., Sugihara, I., Ruigrok, T. J. H., Eisenman, L. M., & Mugnaini, E. (1996). Morphological correlates of bilateral synchrony in the rat cerebellar cortex. *Journal of Neuroscience*, *16*, 3412–3426.

De Zeeuw, C., Simpson, J., Hoogenraad, C., Galjart, N., Koekkoek, S., & Ruigrok, T. (1998). Microcircuitry and function of the inferior olive. *Trends in Neurosciences*, *21*, 391–400.

Flash, T., & Hogan, N. (1985). The coordination of arm movements: an experimentally confirmed mathematical model. *Journal of Neuroscience*, *5*, 1688–1703.

Fujii, H., & Tsuda, I. (2004). Itinerant dynamics of class I^* neurons coupled by gap junctions. *Lecture Notes in Computer Science*, *3146*, 140–160.

Gellman, R., Gibson, A. R., & Houk, J. C. (1985). Inferior olivary neurons in the awake cat: detection of contact and passive body displacement. *Journal of Neurophysiology*, *54*, 40–60.

Gilbert, P. F., & Thach, W. T. (1977). Purkinje cell activity during motor learning. *Brain Research*, *128*, 309–328.

Goldobin, D. S., Teramae, J., Nakao, H., & Ermentrout, G. B. (2010). Dynamics of limit-cycle oscillators subject to general noise. *Physical Review Letters*, *105*, 154101.

Hesslow, G. (1986). Inhibition of inferior olivary transmission by mesencephalic stimulation in the cat. *Neuroscience Letters*, *63*, 76–80.

Hesslow, G., & Ivarsson, M. (1996). Inhibition of the inferior olive during conditioned responses in the decerebrate ferret. *Experimental Brain Research*, *110*, 36–46.

Highstein, S. M., Partsalis, A., & Arikan, R. (1997). Role of the Y-group of the vestibular nuclei and flocculus of the cerebellum in motor learning of the vestibulo-ocular reflex. *Progress in Brain Research*, *114*, 383–397.

Ito, M. (1970). Neurophysiological aspects of the cerebellar motor control system. *International Journal of Neurology*, *7*, 162–176.

Ito, M. (1984). *The cerebellum and neural control*. New York: Raven Press.

Ito, M. (1990). A new physiological concept on cerebellum. *Revue Neurologique (Paris)*, *146*, 564–569.

Ito, M., Sakurai, M., & Tongroach, P. (1982). Climbing fibre induced long term depression of both mossy fibre responsiveness and glutamate sensitivity of cerebellar Purkinje cells. *Journal of Physiology*, *324*, 113–134.

Kaplan, J. L., & Yorke, J. A. (1970). Chaotic behavior of multidimensional difference equations. In H. O. Walter, & H. Peitgen (Eds.), *Lecture notes in mathematics*: *vol. 730. Functional differential equations and approximations of fixed points* (pp. 204–227). Berlin: Springer-Verlag.

Katayama, M., & Kawato, M. (1993). Virtual trajectory and stiffness ellipse during multijoint arm movement predicted by neural inverse models. *Biological Cybernetics*, *69*, 353–362.

Katori, Y., Lang, E. J., Onizuka, M., Kawato, M., & Aihara, K. (2010). Quantitative modeling of spatio-temporal dynamics of inferior olive neurons with a simple conductance-based model. *International Journal of Bifurcation and Chaos*, *20*, 583–603.

Kawato, M., Furukawa, K., & Suzuki, R. (1987). A hierarchical neural-network model for control and learning of voluntary movement. *Biological Cybernetics*, *57*, 169–185.

Kawato, M., & Gomi, H. (1992). A computational model of four regions of the cerebellum based on feedback-error learning. *Biological Cybernetics*, *68*, 95–103.

Kawato, M., Kuroda, S., & Schweighofer, N. (2011). Cerebellar supervised learning revisited: biophysical modeling and degrees-of-freedom control. *Current Opinion in Neurobiology*, *21*, 791–800.

Khater, T. T., Quinn, K. J., Pena, J., Baker, J. F., & Peterson, B. W. (1993). The latency of the cat vestibulo-ocular reflex before and after short and long term adaptation. *Experimental Brain Research*, *94*, 16–32.

Kim, J. J., Krupa, D. J., & Thompson, R. F. (1998). Inhibitory cerebello-olivary projections and blocking effect in classical conditioning. *Science*, *279*, 570–573.

Kitazawa, S., Kimura, T., & Yin, P. B. (1998). Cerebellar complex spikes encode both destinations and error in arm movements. *Nature*, *392*, 494–497.

Kuramoto, Y. (1984). *Chemical oscillations, waves and turbulence*. Berlin: Springer.

Lang, E. J., Sugihara, I., & Llinás, R. (1996). GABAergic modulation of complex spike activity by the cerebellar nucleoolivary pathway in rat. *Journal of Neurophysiology*, *76*, 255–275.

Lidierth, M., & Apps, R. (1990). Gating in the spino-olivocerebellar pathways to the c1 zone of the cerebellar cortex during locomotion in the cat. *Journal of Physiology (London)*, *430*, 453–469.

Lisberger, S. (1988). The neural basis for learning of simple motor skills. *Science*, *242*, 728–735.

Llinás, R., Baker, R., & Sotelo, C. (1974). Electrotonic coupling between neurons in cat inferior olive. *Journal of Neurophysiology*, *37*, 560–571.

Llinás, R., & Yarom, Y. (1981a). Electrophysiology of mammalian inferior olivary neurones in vitro: different types of voltage-dependent ionic conductances. *Journal of Physiology (London)*, *315*, 549–567.

Llinás, R., & Yarom, Y. (1981b). Properties and distribution of ionic conductances generating electroresponsiveness of mammalian inferior olivary neurones in vitro. *Journal of Physiology (London)*, *315*, 569–584.

Llinás, R., & Yarom, Y. (1986). Oscillatory properties of guinea-pig inferior olivary neurones and their pharmacological modulation: an in vitro study. *Journal of Physiology (London)*, *376*, 163–182.

Makarenko, V., & Llinás, R. (1998). Experimentally determined chaotic phase synchronization in a neuronal system. *Proceedings of the National Academy of Sciences of the United States of America*, *95*, 15747–15752.

Manor, Y., Rinzel, J., Segev, I., & Yarom, Y. (1997). Low-amplitude oscillations in the inferior olive: a model based on electrical coupling of neurons with heterogeneous channel densities. *Journal of Neurophysiology*, *77*, 2736–2752.

Marr, D. (1969). A theory of cerebellar cortex. *Journal of Physiology*, *202*, 437–470.

Marshall, S. P., & Lang, E. J. (2009). Local changes in the excitability of the cerebellar cortex produce spatially restricted changes in complex spike synchrony. *Journal of Neuroscience*, *29*, 14352–14362.

Masuda, N., & Aihara, K. (2002). Bridging rate coding and temporal spike coding by effect of noise. *Physical Review Letters*, *88*, 248101.

Masuda, N., & Aihara, K. (2003). Duality of rate coding and temporal coding in multilayered feedforward networks. *Neural Computation*, *15*, 103–125.

Miall, R. C., Christensen, L. O., Cain, O., & Stanley, J. (2007). Disruption of state estimation in the human lateral cerebellum. *PLoS Biology*, *5*, e316.

Miall, R. C., Weir, D. J., Wolpert, D. M., & Stein, J. F. (1993). Is the cerebellum a smith predictor? *Journal of Motor Behavior*, *25*, 203–216.

Nelson, B. J., & Mugnaini, E. (1989). Origins of GABAergic inputs to the inferior olive. In P. Strata (Ed.), *Experimental research series*: *vol. 17*. *The olivocerebellar system in motor control* (pp. 86–87). Berlin: Springer-Verlag.

Oniuzka, M., Hoang, T. H., Kawato, M., Schweighofer, N., Katori, Y., & Aihara, K. (2013). Statistical estimation of gap-junctional and inhibitory conductance in inferior olive neurons by network model simulation using PCA and ANOVA of firing feature vectors. *Neural Networks*.

Onizuka, M., Schweighofer, N., Katori, Y., Aihara, K., Toyama, K., & Kawato, M. (2010). Reproduction of complex spike firing patterns with modulated effective coupling conductance in inferior olive neurons. *Neuroscience Research*, *68*, e435.

Pastor, A. M., De la Cruz, R. R., & Baker, R. (1997). Chapter 21: characterization of Purkinje cells in the goldfish cerebellum during eye movement and adaptive modification of the vestibulo-ocular reflex. *Progress in Brain Research*, *114*, 359–381.

Pikovsky, A., Rosenblum, M., & Kurths, J. (2001). *Synchronization: a universal concept in nonlinear sciences*. Cambridge: Cambridge University Press.

Raymond, J., Lisberger, S. G., & Mauk, M. (1996). The cerebellum: a neuronal learning machine? *Science*, *272*, 1126–1131.

Rényi, A. (1970). *Probability theory*. Amsterdam: North-Holland.

Rössler, O. E. (1979). Continuous chaos. *Annals of the New York Academy of Sciences*, *31*, 376–392.

Schweighofer, N. (1998). A model of activity-dependent formation of cerebellar microzones. *Biological Cybernetics*, *79*, 97–107.

Schweighofer, N., Doya, K., Fukai, H., Chiron, J. V., Furukawa, T., & Kawato, M. (2004). Chaos may enhance information transmission in the inferior olive. *Proceedings of the National Academy of Sciences of the United States of America*, *101*, 4655–4660.

Schweighofer, N., Doya, K., & Kawato, M. (1999). Electrophysiological properties of inferior olive neurons: a compartmental model. *Journal of Neurophysiology*, *82*, 804–817.

Schweighofer, N., Doya, K., & Lay, F. (2001). Unsupervised learning of granule cell sparse codes enhances cerebellar adaptive control. *Neuroscience*, *103*, 35–50.

Schweighofer, N., Spoelstra, J., Arbib, M. A., & Kawato, M. (1998). Role of the cerebellum in reaching movements in humans. II. A neural model of the intermediate cerebellum. *European Journal of Neuroscience*, *10*, 95–105.

Shidara, M., Kawano, K., Gomi, H., & Kawato, M. (1993). Inverse-dynamics model eye movement control by Purkinje cells in the cerebellum. *Nature*, *365*, 50–52.

Shimada, I., & Nagashima, T. (1979). A numerical approach to ergodic problem of dissipative dynamical systems. *Progress of Theoretical Physics*, *61*, 1605–1616.

Teramae, J., & Tanaka, D. (2004). Robustness of the noise-induced phase synchronization in a general class of limit cycle oscillators. *Physical Review Letters*, *93*, 204103.

Thompson, R. F., Thompson, J. K., Kim, J. J., Krupa, D. J., & Shinkman, P. G. (1998). The nature of reinforcement in cerebellar learning. *Neurobiology of Learning and Memory*, *70*, 150–176.

Tokuda, I., Han, K., Aihara, K., Kawato, M., & Schweighofer, N. (2010). The role of chaotic resonance in cerebellar learning. *Neural Networks*, *23*, 836–842.

Tseng, Y. W., Diedrichsen, J., Krakauer, J. W., Shadmehr, R., & Bastian, A. J. (2007). Sensory prediction errors drive cerebellum-dependent adaptation of reaching. *Journal of Neurophysiology*, *98*, 54–62.

Tsuda, I., Fujii, H., Tadokoro, S., Yasuoka, T., & Yamaguchi, Y. (2004). Chaotic itinerancy as a mechanism of irregular changes between synchronization and desynchronization in a neural network. *Journal of Integrative Neuroscience*, *3*, 159–182.

Uusisaari, M., & De Schutter, E. (2011). The mysterious microcircuitry of the cerebellar nuclei. *Journal of Physiology*, *589*, 3441–3457.

Van Der Giessen, R. S., Koekkoek, S. K., Van Dorp, S., De Gruijl, J. R., Cupido, A., & Khosrovani, S. (2008). Role of olivary electrical coupling in cerebellar motor learning. *Neuron*, *58*, 599–612.

Van Essen, T. A., Van der Giessen, R. S., Koekkoek, S. K. E., Van der Werf, F., De Zeeuw, C. I., & Van Genderen, P. J. J. (2010). Anti-malaria drug mefloquine induces motor learning deficits in humans. *Frontiers in Neuroscience*, *4*, 191.

Van Kan, P. L., Gibson, A. R., & Houk, J. C. (1993). Movement-related inputs to intermediate cerebellum of the monkey. *Journal of Neurophysiology*, *69*, 74–94.